Asymmetric behavior of current-induced magnetization switching in a magnetic tunnel junction: Non-equilibrium first-principles calculations

Applied Physics Express **7**, 045202 (2014)
http://dx.doi.org/10.7567/APEX.7.045202

Asymmetric behavior of current-induced magnetization switching in a magnetic tunnel junction: Non-equilibrium first-principles calculations

Masaaki Araidai[1*], Takahiro Yamamoto[2], and Kenji Shiraishi[3,4]

[1]*Department of Quantum Engineering, Graduate School of Engineering, Nagoya University, Nagoya 464-8603, Japan*
[2]*Department of Liberal Arts (Physics), Faculty of Engineering, Tokyo University of Science, Katsushika, Tokyo 125-8585, Japan*
[3]*Department of Computational Science and Engineering, Graduate School of Engineering, Nagoya University, Nagoya 464-8603, Japan*
[4]*Faculty of Pure and Applied Sciences, University of Tsukuba, Tsukuba, Ibaraki 305-8571, Japan*
E-mail: araidai@cse.nagoya-u.ac.jp

Received February 6, 2014; accepted February 19, 2014; published online March 10, 2014

We investigated the microscopic mechanisms of current-induced magnetization switching (CIMS) in an Fe/MgO(001)/Fe/Ta magnetic tunnel junction using non-equilibrium first-principles calculations. We found that the change in the magnetization configuration from antiparallel (AP) to parallel (P) can be realized with a lower electrical power than that from P to AP. From detailed analyses of the density of states subject to a finite bias voltage, we clarified that the asymmetric behavior originates from the difference in the electron scattering processes between switching directions.

Investigating magnetic tunnel junctions (MTJs) is of key importance for the development of advanced magnetoresistive random access memory (MRAM).[1–3] An MTJ consisting of two metal ferromagnets separated by a thin insulator is the minimum unit that exhibits the tunnel magnetoresistance (TMR) effect, which is a variation in the resistance depending on whether the relative directions of the ferromagnet magnetizations are parallel (P) or antiparallel (AP). The simplest way to switch a magnetization configuration is by using external magnetic fields. However, the absolute currents required for magnetic field switching do not scale when the junction size is reduced.[4] On the other hand, current-induced magnetization switching (CIMS), which is due to the spin-transfer torque,[5] does exhibit scalability, and for that reason is drawing attention as one of the most promising candidates for magnetization switching.[4,6,7]

CIMS has been successfully applied to the operation of MRAM devices with a lower power, and it enables the development of large-capacity MRAM devices because it enables further miniaturization. At the same time, the device properties have been greatly influenced by various microscopic factors, which has been clearly observed as the asymmetry of the critical current.[8,9] The asymmetric behavior is considered to be the result of various effects, such as the difference in the magnetic dipole–dipole interactions[9,10] and interfacial perpendicular magnetic anisotropy due to the electric field.[11] In addition, it may be caused by the difference in the densities of states (DOSs) depending on the polarity of the bias voltage. Although the DOS based on non-equilibrium electronic states directly affects the electron scattering processes, it has not yet been studied well. Accordingly, we investigate CIMS in an MTJ using non-equilibrium first-principles calculations. Although some first-principles studies have investigated the spin-transfer torque,[12,13] fully non-equilibrium calculations have not yet been performed. This is the first report on non-equilibrium first-principles calculations for CIMS in an MTJ to the best of our knowledge.

To precisely calculate the current–voltage characteristics of an MTJ with a magnetization configuration, we employed the commercially available Atomistix ToolKit,[14] which is a simulation package based on the non-equilibrium Green's function technique combined with density functional theory.[15] This code adopts pseudo-atomic orbitals (PAOs) as basis functions[16] and norm-conserving pseudopotentials as interaction potentials between electrons and ions.[17] We employed single-zeta polarized orbitals as the PAOs and the local density approximation as the exchange–correlation potential.[18] Magnetic dipole–dipole interactions and the interfacial perpendicular magnetic anisotropy are not explicitly included in these calculations owing to the lack of Breit[19] and spin–orbit interactions. Only the contributions derived from non-equilibrium electronic states are taken into account.

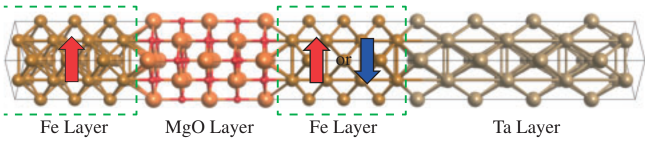

Fig. 1. Calculation model of an Fe/MgO(001)/Fe MTJ with a paramagnetic Ta lead. Open boundary conditions are imposed in the direction normal to the layers to treat electron flow, and periodic boundary conditions are imposed in the directions parallel to the layers. The magnetization in the attached iron electrode is fixed at the bulk value, and that in the thin iron layer is optimized according to the tunneling current through the junction.

We employed an Fe/MgO(001)/Fe MTJ with a tantalum electrode, as shown in Fig. 1, as the calculation model. CoFe layers with a strong interfacial perpendicular magnetic anisotropy were employed recently to decrease the magnitude of the critical currents for magnetization switching. However, the electronic states of the CoFe layers around the Fermi level are essentially similar to those of Fe layers: conducting *s* electrons and itinerant d electrons. Therefore, the study of an MTJ with Fe layers is sufficient for understanding the nature of the asymmetric behavior. Moreover, because the TMR of an Fe/MgO/Fe MTJ has been extensively investigated theoretically,[20–23] we can focus solely on clarifying the asymmetric behavior in CIMS. A semi-infinite iron electrode with a spin polarization fixed at the optimized value is attached to the left side of the leftmost iron layers, and a paramagnetic tantalum electrode is attached to the right side of the rightmost tantalum layers. Periodic boundary conditions are imposed in the directions parallel to the layers. Once the optimal electron density distribution between the electrodes is obtained, depending on the initial spin configuration and applied bias voltage, we can determine the optimal magnetization configuration in the MTJ. The current–voltage characteristics of the model are shown in

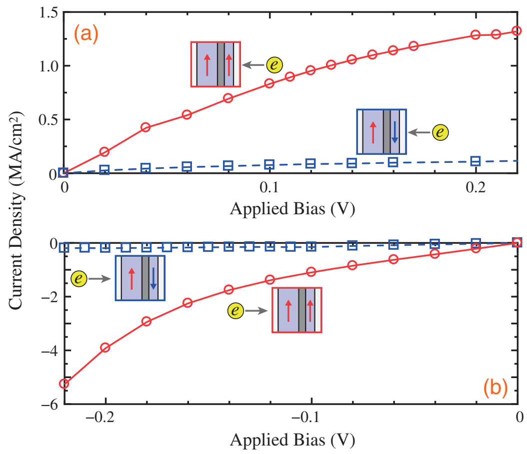

Fig. 2. Electric-current densities for (a) positive and (b) negative bias voltages. Solid and dashed lines denote current densities with P and AP magnetization configurations, respectively. Insets show schematic diagrams of magnetization configuration and electron flow.

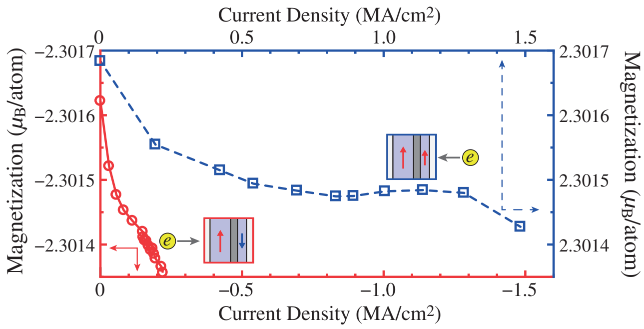

Fig. 3. Average magnetization over atoms in magnetization switching layer as a function of electric current density. Solid and dashed lines denote magnetization with AP configuration for negative bias and P configuration for positive bias, respectively.

Fig. 2. The solid and dashed lines denote the electric currents in the P and AP magnetization configurations, respectively. It is obvious from Fig. 2 that our Fe/MgO/Fe MTJ exhibits very high TMR. The value of the TMR ratio around zero bias is about 626% with an optimistic definition. Such a high TMR in the Fe/MgO/Fe MTJ is consistent with previous experimental and theoretical observations.[20,21,24,25] Additionally, the agreement of our results for the order of the current density with experimental observations is worthy of attention.[9,26]

Here, it must be noted that in the present calculation method, the electron spins were treated collinearly.[27] Because of this treatment, perfect magnetization switching cannot be achieved in the present calculations. However, we can successfully capture the precursors, which allows us to determine the details of the CIMS process. It is experimentally observed that the AP configuration is switched to the P configuration at the critical current for negative bias, and the P configuration is switched to the AP configuration at the critical current for positive bias. Therefore, we focus on the AP magnetization configuration for negative bias [dashed line in Fig. 2(b)] and the P configuration for positive bias [solid line in Fig. 2(a)]. The former and latter correspond to the initial configuration when the configuration changes from AP to P and from P to AP, respectively.

Figure 3 shows the average magnetization over atoms in the magnetization switching layer as a function of the electric current density. The solid and dashed lines correspond to the AP configuration for negative bias and the P configuration forpositive bias, respectively. There are two major findings from Fig. 3. One is that in both cases, the magnetization corresponding to the majority spin in the switching layer decreases with increasing current density through the junction, which indicates the onset of magnetization switching. The other is that the decreasing rate of magnetization in the AP configuration for negative bias (solid line in Fig. 3) is much larger than that in the P configuration for positive bias (dashed line in Fig. 3), which means that the AP-to-P case can be realized with a lower electrical power than the P-to-AP case. The qualitative features are in good agreement with experimental observations.[9]

Our two theoretical observations can be rationalized from detailed analyses using the DOS subject to a finite bias voltage, which is directly responsible for the scattering processes of electrons flowing through the MTJ. We begin with the CIMS from the AP-to-P magnetization configurations and then proceed to that from the P-to-AP configurations. The diagram of the DOS in the AP configuration for negative bias is shown in Fig. 4(a). In the AP-to-P case, electrons come from deep inside the left iron electrode toward the right tantalum electrode. The number of spin-up electrons is originally larger than that of spin-down electrons because of the spin polarization in the iron electrode. When the bias voltage is small [the upper panel in Fig. 4(a)], the number of spin-up (-down) states in the electrode within the bias window is large (small), whereas the number of spin-up (-down) states in the unoccupied states in the switching layer is small (large), leading to suppression of the tunnel currents in the AP configuration. When the bias voltage becomes larger [the lower panel in Fig. 4(a)], the unoccupied states of spin-up electrons in the switching layer enter the bias window, and many conduction electrons with up spin pass through the switching layer. As a result, owing to Hund's coupling between the conduction electrons with up spin and the magnetization parallel to down spin in the switching layer, the magnetization configuration in the MTJ can be switched from the AP configuration to the P configuration.

Figure 4(b) represents the DOS of the P configuration for positive bias. The main difference from the AP-to-P case is that spin-*unpolarized* electron currents come from the paramagnetic tantalum electrode toward the ferromagnetic iron electrode through the magnetization switching layer, which is thin enough to allow tunneling. When the bias voltage is small [the upper panel in Fig. 4(b)], many of the up-spin electrons flow through the MTJ because there are many states with up spin in both the iron electrode and the switching layer. On the other hand, many of the down-spin electrons are reflected at the switching layer, but some of them tunnel through. Most of the tunneling electrons with down spin, however, are reflected at the iron electrode because few unoccupied states with down spin are available in the electrode. When the reflected electrons return to the switching layer, most of them are reflected again because of the small number of down-spin states. Considering the magnetization behavior shown in Fig. 3, which exhibits a relative increase in the minority spin in the switching layer,

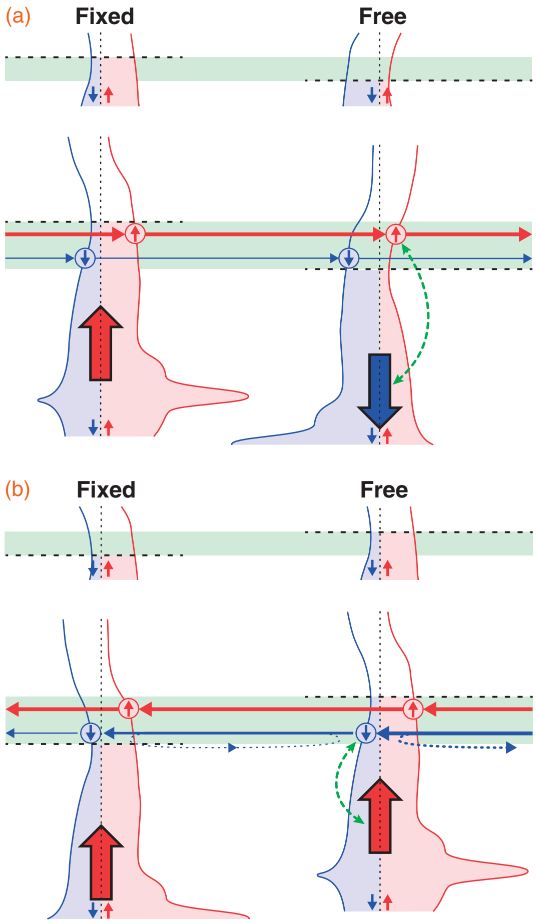

Fig. 4. DOS at iron electrode (left) and magnetization switching layer (right) subject to a finite bias voltage: (a) AP configuration for negative bias and (b) P configuration for positive bias. The shape of the DOS is based on the calculation results but has been simplified for clarity. Upper and lower panels in (a) and (b) correspond to low bias voltage and higher bias voltage, respectively. In (a) and (b), the shaded bands denote the bias windows, and the shaded areas in the DOS represent the occupied states. The large arrows in the DOS denote the total magnetization at the electrode and the switching layer, and the arrows within the bias window in the lower panels indicate the flow of spin-up and spin-down electrons. The width of these arrows indicates the absolute magnitude of the electron currents. The dashed lines with arrows at both ends represent Hund's coupling between conduction electrons and electrons in occupied states in the switching layer. In (b), the dotted lines with an arrow at the end denote the reflections of spin-down electrons.

together with the electron flows described above, we can suggest that multiple reflections occur between the switching layer and the iron electrode. These multiple reflections in the steady flow of spin-down electrons stimulate the magnetization switching. The reflections are indicated by the dotted line in the lower panel in Fig. 4(b). At a higher bias [the lower panel in Fig. 4(b)], the electric current of spin-up electrons is saturated by the disappearance of the unoccupied states in the iron electrode, and that of spin-down electrons increases monotonically because both the unoccupied states in the electrode and the occupied states in the switching layer enter the bias window. Because of the multiple reflections and the increase in conduction electrons with down spin through the switching layer, the magnetization of the switching layer can be switched by Hund's coupling.

In summary, CIMS in an Fe/MgO(001)/Fe MTJ was investigated through first-principles calculations. This study is the first effort to examine CIMS through fully non-equilibrium calculations. A large TMR ratio was obtained even for an MTJ model with a tantalum paramagnetic electrode. The magnitude of the electric current density required for magnetization switching in the AP-to-P case was lower than that required for the P-to-AP case. From detailed analyses of the DOS subject to a finite bias voltage, we clarified that the origin of the asymmetric magnetization switching behavior is the difference in the electron scattering processes between the switching directions.

Acknowledgment One of the authors (M.A.) acknowledges fruitful discussions with Masahito Tsujikawa.

1) E. Y. Tsymbal, O. N. Mryasov, and P. R. LeClair, J. Phys.: Condens. Matter **15**, R109 (2003).
2) C. Heiliger, P. Zahn, and I. Mertig, Mater. Today **9** [11], 46 (2006).
3) S. Yuasa and D. D. Djayaprawira, J. Phys. D **40**, R337 (2007).
4) S. Ikeda, J. Hayakawa, Y. M. Lee, F. Matsukura, Y. Ohno, T. Hanyu, and H. Ohno, IEEE Trans. Magn. **46**, 1873 (2010).
5) D. C. Ralph and M. D. Stiles, J. Magn. Magn. Mater. **320**, 1190 (2008).
6) J. C. Slonczewski, J. Magn. Magn. Mater. **159**, L1 (1996).
7) L. Berger, Phys. Rev. B **54**, 9353 (1996).
8) Y. Saito, T. Inokuchi, H. Sugiyama, and K. Inomata, Eur. Phys. J. B **59**, 463 (2007).
9) S. Ikeda, K. Miura, H. Yamamoto, K. Mizunuma, H. D. Gan, M. Endo, S. Kanai, J. Hayakawa, F. Matsukura, and H. Ohno, Nat. Mater. **9**, 721 (2010).
10) H. Sato, M. Yamanouchi, K. Miura, S. Ikeda, H. D. Gan, K. Mizunuma, R. Koizumi, F. Matsukura, and H. Ohno, Appl. Phys. Lett. **99**, 042501 (2011).
11) W. G. Wang and C. L. Chien, J. Phys. D **46**, 074004 (2013).
12) P. M. Haney, D. Waldron, R. A. Duine, A. S. Núñez, H. Guo, and A. H. MacDonald, Phys. Rev. B **76**, 024404 (2007).
13) C. Heiliger and M. D. Stiles, Phys. Rev. Lett. **100**, 186805 (2008).
14) QuantumWise HP [http://www.quantumwise.com/].
15) M. Brandbyge, J.-L. Mozos, P. Ordejón, J. Taylor, and K. Stokbro, Phys. Rev. B **65**, 165401 (2002).
16) J. Junquera, Ó. Paz, D. Sánchez-Portal, and E. Artacho, Phys. Rev. B **64**, 235111 (2001).
17) N. Troullier and J. L. Martins, Phys. Rev. B **43**, 1993 (1991).
18) J. P. Perdew and A. Zunger, Phys. Rev. B **23**, 5048 (1981).
19) S. Bornemann, J. Minár, J. Braun, D. Ködderitzsch, and H. Ebert, Solid State Commun. **152**, 85 (2012).
20) W. H. Butler, X.-G. Zhang, T. C. Schulthess, and J. M. MacLaren, Phys. Rev. B **63**, 054416 (2001).
21) J. Mathon and A. Umerski, Phys. Rev. B **63**, 220403(R) (2001).
22) I. Rungger, O. Mryasov, and S. Sanvito, Phys. Rev. B **79**, 094414 (2009).
23) X. Feng, O. Bengone, M. Alouani, S. Lebègue, I. Rungger, and S. Sanvito, Phys. Rev. B **79**, 174414 (2009).
24) S. S. P. Parkin, C. Kaiser, A. Panchula, P. M. Rice, B. Hughes, M. Samant, and S.-H. Yang, Nat. Mater. **3**, 862 (2004).
25) S. Yuasa, T. Nagahama, A. Fukushima, Y. Suzuki, and K. Ando, Nat. Mater. **3**, 868 (2004).
26) E. Chen, D. Apalkov, Z. Diao, A. Driskill-Smith, D. Druist, D. Lottis, V. Nikitin, X. Tang, S. Watts, S. Wang, S. A. Wolf, A. W. Ghosh, J. W. Lu, S. J. Poon, M. Stan, W. H. Butler, S. Gupta, C. K. A. Mewes, T. Mewes, and P. B. Visscher, IEEE Trans. Magn. **46**, 1873 (2010).
27) When electron spins are treated collinearly, the rotation of the magnetization vector cannot be described directly. Instead, the rotation can be expressed as the change in the length of the magnetization vector. Because of this suppression of the degrees of freedom, self-consistent calculations at bias voltages greater than 0.25 V become extremely unstable.